JOURNAL OF COMPUTATIONAL PHYSICS 9, 10–25 (1972)

Evolution of a Stationary Disk of Stars

FRANK HOHL

NASA Langley Research Center, Hampton, Virginia 23365

Received April 8, 1971

An improved potential solver for calculating the gravitational potential of isolated disk galaxies is presented. The potential solver is used to investigate the evolution of initially stationary axisymmetric disks of stars for various values of the initial velocity dispersion.

I. INTRODUCTION

Two computer models for "collisionless" self-gravitating thin disk galaxies have recently been described by Miller and Prendergast [1] and by Hohl and Hockney [2]. To obtain the gravitational potential or force in these models, an $n \times n$ array of cells is superposed over the galactic disk. The mass density in each of the $n \times n$ cells is used to obtain the gravitational force by means of convolution methods making use of fast Fourier transforms [3]. Because of the periodic nature of finite Fourier transforms, Miller et al. [1,4] used a doubly periodic model for their force calculations. Hohl and Hockney [2] modified the Fourier transform method to obtain the potential for isolated disk galaxies. However, to obtain the gravitational potential for an isolated disk galaxy covering an $n \times n$ array of cells, the Fourier transforms were performed on an $2n \times 2n$ array of cells, thereby increasing the required storage for the potential calculation by a factor of four. In the present paper a modified potential solver is presented which allows the potential for isolated disk galaxies to be obtained with only a twofold increase in storage.

In published work [1, 2, 4—6] on the simulation of disk galaxies, the initial conditions chosen were not solutions of the time-independent collisionless Boltzman equation. Even though some of the initial conditions [5, 6] were for initially balanced disks, these initial conditions did not correspond to stationary disks. One exception to this is the "cold" balanced disk which, however, is violently unstable. In the present paper, the evolution of initially stationary disks for various temperatures is investigated. With the exception of the modified potential solver the model used for the calculations is the same as that presented previously [2].

II. Potential Calculation

The scaled gravitational potential at the center of cell (x, y) is defined by the double summation over the two-dimensional array of cells

$$\phi_{x,y} = \sum_{i=0}^{N-1} \sum_{j=0}^{N-1} \mu_{i,j} H_{i-x,j-y}\,, \tag{1}$$

where

$$H_{i,j} = (i^2 + j^2)^{-1/2} \quad \text{for} \quad i + j \neq 0,$$
$$H_{0,0} = 1,$$

and $\mu_{i,j}$ is the mass density in cell (i, j). The double summation is evaluated by the convolution method using fast Fourier transforms [2]. That is, the Fourier transform of the potential equals the product of the Fourier transforms of μ and H

$$\tilde{\phi}_{k,l} = \tilde{\mu}_{k,l} \tilde{H}_{k,l}\,. \tag{2}$$

The gravitational potential $\phi_{x,y}$ is obtained by taking the inverse Fourier transform of (2). Rather than using a complex Fourier series, we have chosen to use a real expansion. For example, the Fourier transform of the density $\mu_{x,y}$ is given by

$$\begin{aligned}
\tilde{\mu}_{k,l} &= \sum_{y=0}^{N-1} \sum_{x=0}^{N-1} c(x)\, c(y)\, \mu_{x,y} \cos(\pi k x/n) \cos(\pi l y/n) && 0 \leqslant k, l \leqslant n \\
&= \sum_{y=0}^{N-1} \sum_{x=0}^{N-1} c(x)\, \mu_{x,y} \cos(\pi k x/n) \sin[\pi(l - n)\, y/n] && \begin{array}{l} 0 \leqslant k \leqslant n \\ n < l < N \end{array} \\
&= \sum_{y=0}^{N-1} \sum_{x=0}^{N-1} c(y)\, \mu_{x,y} \sin[\pi(k - n)\, x/n] \cos(\pi l y/n) && \begin{array}{l} n < k < N \\ 0 \leqslant l \leqslant n \end{array} \\
&= \sum_{y=0}^{N-1} \sum_{x=0}^{N-1} \mu_{x,y} \sin[\pi(k - n)\, x/n] \sin[\pi(l - n)\, y/n], && n < k, l < N
\end{aligned} \tag{3}$$

where

$$c(x) = 1/\sqrt{2} \text{ if } x = 0 \quad \text{or} \quad x = n,$$
$$c(x) = 1, \text{ otherwise,}$$

n defines the $n \times n$ active array and $N = 2n$ defines the larger array over which the Fourier transform must be taken so that the potential for an isolated disk galaxy is obtained. Note that the density may be nonzero only in the smaller $n \times n$

array. Because of the symmetry of $H_{x,y}$, the Fourier transform $\tilde{H}_{k,l}$ can be obtained by a finite cosine transform

$$\tilde{H}_{k,l} = \sum_{y=0}^{n} \sum_{x=0}^{n} c^2(x)\, c^2(y)\, H_{x,y} \cos(\pi kx/n) \cos(\pi ly/n), \qquad 0 \leqslant k, l \leqslant n, \quad (4)$$

and

$$\tilde{H}_{k+n,l} = \tilde{H}_{k,l+n} = \tilde{H}_{k+n,l+n} = \tilde{H}_{k,l}\,.$$

The next step in obtaining the potential is to multiply $\tilde{\mu}_{k,l}$ by $\tilde{H}_{k,l}$ to obtain

$$\tilde{\phi}_{k,l} = \tilde{\mu}_{k,l} \tilde{H}_{k,l}\,. \quad (5)$$

The gravitational potential for an isolated galaxy correctly defined over the $n \times n$ array is obtained by the Fourier synthesis

$$\begin{aligned} \phi_{x,y} = \frac{1}{N^2} \Bigg[& \sum_{l=0}^{n} \left\{ \sum_{k=0}^{n} \tilde{\phi}_{k,l} \cos\left(\frac{\pi}{n} kx\right) + \sum_{k=n+1}^{N-1} \tilde{\phi}_{k,l} \sin\left(\frac{\pi}{n} (k-n)\, x\right) \right\} \\ & \times \cos\left(\frac{\pi}{n} ly\right) \\ & + \sum_{l=n+1}^{N-1} \left\{ \sum_{k=0}^{n} \tilde{\phi}_{k,l} \cos\left(\frac{\pi}{n} kx\right) + \sum_{k=n+1}^{N-1} \tilde{\phi}_{k,l} \sin\left(\frac{\pi}{n} (k-n)\, x\right) \right\} \\ & \times \sin\left(\frac{\pi}{n} (l-n)\, y\right) \Bigg]. \end{aligned} \quad (6)$$

Table I gives a Fortran listing of the computer program actually used to obtain the potential by use of an $N \times n$ array of cells. The variable 12A defines the size of the rectangular array used for the potential calculation. When the subroutine GETPHI is called, RHO(I, J) contains the mass density and GETPHI places the values of the corresponding gravitational potential in RHO(I, J). The subroutine FTRANS (I,I2B) has been written by R. Hockney [7] and it performs a finite Fourier analysis or synthesis on the common input array Z and places the result in the common output array Y. The subroutine performs a cosine analysis for I = 2, a periodic analysis for I = 3, and a periodic synthesis for I = 4. The subroutine GETSET (I, I2B) initializes FTRANS and is called every time the arguments of FTRANS (I, I2B) are changed. The Fourier transform $H_{k,l}$ is calculated on an $(n+1) \times (n+1)$ array only the first time that the subroutine is called and is kept in storage for subsequent use.

We next obtain the Fourier transform of $\mu_{x,y}$ in the x-direction on the $N \times n$ array, that is, for $0 \leqslant x \leqslant N-1$ and $0 \leqslant y \leqslant n$. Since $\mu_{x,y}$ is nonzero only over the $n \times n$ array, the components of the Fourier transform of $\mu_{x,y}$ in the x-direction

TABLE I

Subroutine for Calculating The Gravitational Potential

```
      SUBROUTINE GETPHI
      COMMON Z(257),Y(257),RHO(256,128),12A,
        ITEST
      DIMENSION H(129,129)
      IF(ITEST.EQ.O) GO TO 10
      ITEST=0
      I2B=I2A-1
      N=2**12A
      N02=N/2
      N21=N02+1
      RNI=1./(N*N)
      DO 1 J=1, N21
      DO 1 I=1, N21
      IF(I.EQ.1.AND.J.EQ.1) GO TO 1
      H(I,J)=RNI/SQRT((I-1.)*(I-1.)+(J-1.)*(J-1.))
    1 CONTINUE
      H(1,1)=RNI
      CALL GETSET(2,I2B)
      DO 2 J=1,N21
      DO 3 I-1,N21
    3 Z(I)=H(I, J)
      CALL FTRANS(2,I2B)
      DO 4 I=1, N21
    4 H(I,J)=Y(I)
    2 CONTINUE
      DO 5 I=1,N21
      DO 6 J=1,N21
    6 Z(J)=H(I,J)
      CALL FTRANS(2,I2B)
      DO 7 J=1,N21
    7 H(I,J)=Y(J)
    5 CONTINUE
   10 CONTINUE
      CALL GETSET(3,I2A)
      DO 11 J=1,N02
      DO 8 I=1,N
    8 Z(I)=RHO(I,J)
      CALL FTRANS(3,I2A)
      DO 9 I=1, N
    9 RHO(I,J)=Y(I)
   11 CONTINUE
      DO 12 I=1,N
      DO 13 J=1, N02
      Z(J)=RHO(I,J)
   13 Z(J+N02)=0.
      CALL GETSET(3,I2A)
      CALL FTRANS(3,I2A)
      IF(I.GT.N21) GO TO 14
      DO 15 J=2,N02
      Z(J)=Y(J)*H(I,J)
   15 Z(J+N02)=Y(J+N02)*H(I,J)
      Z(1)=Y(1)*H(I,1)
      Z(N21)=Y(N21)*H(I,N21)
      GO TO 16
   14 DO 17 J=2,N02
      Z(J)=Y(J)*H(I-N02,J)
   17 Z(J+N02)=Y(J+N02)*H(I-N02, J)
      Z(1)=Y(1)*H(I-N02,1)
      Z(N21)=Y(N21)*H(I-N02,N21)
   16 CONTINUE
      CALL GETSET(4,I2A)
      CALL FTRANS(4,I2A)
      DO 18 J=1, N02
   18 RHO(I,J)=Y(J)
   12 CONTINUE
      DO 19 J=1,N02
      DO 20 I=1,N
   20 Z(I)=RHO(I,J)
      CALL FTRANS(4,I2A)
      DO 21 I=1, N21
   21 RHO(I,J)=Y(I)
   19 CONTINUE
      RETURN
      END
```

will be zero for $n < y < N$. Therefore, by use of the one-dimensional arrays Y and Z we can perform the Fourier transform in the y direction, multiply the result by $\tilde{H}_{k,l}$, and take the inverse Fourier transform in the y-direction. The result is placed in the $N \times n$, RHO(I, J) array for $0 \leqslant y \leqslant n-1$ and $0 \leqslant x \leqslant N-1$ with the values for $n < y < N$ discarded. The final step is to perform the inverse

Fourier transform in the x-direction for $0 \leqslant y \leqslant n - 1$. This procedure gives the correct gravitational potential for an isolated disk galaxy over the $n \times n$ array.

Table II gives the measured time for calculating the gravitational potential with the program listed in Table I. Also shown are the times required for the previous potential solver which required a larger $N \times N$ array. A listing of that program is given elsewhere [6].

TABLE II
Computer Time Required to Obtain The Gravitational Potential

Active $n \times n$ mesh	CDC 6600 CPU Seconds			
	Present potential solver using $2(n \times n)$ storage		Previous potential solver using $4(n \times n)$ storage	
	$\tilde{H}$ calculated	$\tilde{H}$ given	$\tilde{H}$ calculated	$\tilde{H}$ given
16×16	0.164	0.126	0.182	0.144
32×32	.618	.476	.660	.526
64×64	2.440	1.892	2.626	2.086
128×128	10.000	7.740	10.794	8.530

III. Self-Consistent Stationary Disks

A time-independent, axisymmetric self-consistent disk of stars is described by the collisionless Boltzmann equation

$$v_r \frac{\partial f}{\partial r} + \frac{v_\theta^2}{r} \frac{\partial f}{\partial v_r} - \frac{v_r v_\theta}{r} \frac{\partial f}{\partial v_\theta} + K_r \frac{\partial f}{\partial v_r} = 0, \tag{7}$$

where v_r and v_θ are the radial and azimuthal velocity components and $f(r, v_r, v_\theta)$ is the distribution function such that

$$dm = f(r, v_r, v_\theta)\, dv_r\, dv_\theta\, r dr d\theta \tag{8}$$

corresponds to the mass in a surface element $r dr d\theta$. The gravitational field K_r equals $\partial\phi/\partial r$, where the potential $\phi(r, z)$ is obtained from the Poisson equation

$$\nabla^2\phi = 4\pi G\mu(r)\, \delta(z), \tag{9}$$

where G is the gravitational constant and the density $\mu(r)$ is given by

$$\mu(r) = \iint f(r, v_r, v_\theta)\, dv_r\, dv_\theta\,. \tag{10}$$

According to Jean's Theorem [8, 9] any function of the form

$$f(r, v_r, v_\theta) = f(E, J) \tag{11}$$

is a solution of Eq. (7), where the energy E and the angular momentum J are given by

$$E = \tfrac{1}{2}(v_r^2 + v_\theta^2) + \phi,$$

and

$$J = rv_\theta,$$

respectively.

The uniformly rotating disk with a mass density variation given by

$$\mu(r) = \mu(0)\sqrt{1 - r^2/R^2} \tag{12}$$

has been extensively used in numerical simulations of disk galaxies [6, 2]. In Eq. (10) $\mu(0)$ is the central mass density and R is the radius of the disk. The gravitational potential inside the disk is [6]

$$\phi(r) = \tfrac{1}{2}\omega_0^2 r^2 - \omega_0^2 R^2, \tag{13}$$

where $\omega_0 = \pi\sqrt{G\mu(0)/2R}$ is the uniform angular velocity required to balance the cold (zero velocity dispersion) disk. Omitting the constant term in Eq. (13) we can write

$$2E = \omega_0^2 r^2 + v_r^2 + v_\theta^2. \tag{14}$$

Consider now a distribution function of the form [10]

$$f(E, J) = C_1(C_2 - 2E + 2\omega J)^{-1/2}, \tag{15}$$

where ω is the constant angular velocity of the disk, constraint such that $0 \leqslant \omega \leqslant \omega_0$. We need

$$C_2 - 2E + 2\omega J \geqslant 0;$$

thus, for $r = R$, $v_r = 0$, and $v_\theta = R\omega$ we obtain

$$C_2 - \omega_0^2 R^2 - \omega^2 R^2 + 2\omega^2 R^2 = 0,$$

or

$$C_2 = (\omega_0^2 - \omega^2) R^2. \tag{16}$$

Substituting for E, J, and C_2, we can write Eq. (16) as

$$\begin{aligned} f(E, J) &= C_1[(\omega_0^2 - \omega^2) R^2 - 2E + 2\omega J]^{-1/2} \\ &= C_1[(\omega_0^2 - \omega^2)(R^2 - r^2) - v_r^2 - (v_\theta - r\omega)^2]^{-1/2}. \end{aligned}$$

From Eq. (10) we find

$$\mu(r) = \iint f(E, J)\, dv_r\, dv_\theta$$

$$= 2\pi R C_1 \sqrt{\omega_0^2 - \omega^2}\, \sqrt{1 - r^2/R^2}\,.$$

Therefore, since $\mu(r) = \mu(0)\sqrt{1 - r^2/R^2}$, we obtain

$$C_1 = \frac{\mu(0)}{2\pi R \sqrt{\omega_0^2 - \omega^2}}$$

and finally

$$f(E, J) = f(r, v_r, v_\theta)$$

$$= \frac{\mu(0)}{2\pi R \sqrt{\omega_0^2 - \omega^2}} [(\omega_0^2 - \omega^2)(R^2 - r^2) - v_r^2 - (v_\theta - r\omega)^2]^{-1/2}. \quad (17)$$

The distribution function (17) is a stationary solution of the Boltzmann Eq. (7) and has previously been obtained by Kalnajs [11]. If $\omega = \omega_0$ in Eq. (17) we have the cold, violently unstable disk which was previously investigated [2, 6]. For $\omega = 0$ the disk is nonrotating and purely pressure supported.

Toomre [12] has investigated the stability of a stellar disk by means of a local theory. He estimates that for a disk with a Gaussian velocity distribution, a velocity dispersion equal to, or greater than

$$\sigma_{r,\min} = 3.36\, G\mu/\kappa \quad (18)$$

should be locally stabilizing for exponentially growing axisymmetric modes. In Eq. (18), κ denotes the local value of the epicyclic frequency, which for the uniformly rotating disk is

$$\kappa = 2\omega_0\,.$$

Toomre's evaluation of $\sigma_{r,\min}$ is not easily extended to the present non-Gaussian velocity distribution given by Eq. (17). Also, overstabilities may be present since the density of stars in phase space is not a decreasing function of epicyclic amplitude [13]. Nevertheless, Eq. (18) should represent the local criterion for squelching axisymmetric exponentially growing modes [14]. We therefore consider a parameter Q which is the ratio of the *rms* velocity σ_r of the disk to $\sigma_{r,\min}$ as given by

Eq. (18). We would expect $Q = 1$ to be a lower bound on the *rms* velocities needed for stability. Using $f(r, v_r, v_\theta)$ as given by Eq. (17), we obtain

$$\sigma_\theta^2 + \sigma_r^2 = 2\sigma_r^2 = \frac{1}{\mu(r)} \iint (v_r^2 + (v_\theta - r\omega)^2) f(r, v_r, v_\theta)\, dv_r\, dv_\theta$$

$$= \frac{2}{3} (\omega_0^2 - \omega^2)(R^2 - r^2),$$

or

$$\sigma_r = [(\omega_0^2 - \omega^2)(R^2 - r^2)/3]^{1/2}. \tag{19}$$

For the uniformly rotating disk, Eq. (18) takes the form

$$\sigma_{r,\min} = 0.341\omega_0 \sqrt{R^2 - r^2},$$

so that

$$Q = \sigma_r/\sigma_{r,\min} = 1.69 \sqrt{1 - (\omega/\omega_0)^2}. \tag{20}$$

The variation of Q as a function of ω for the uniformly rotating disk is shown in Fig. 1. The value of Q varies from zero, for $\omega = \omega_0$, to 1.69 for $\omega = 0$. Q is equal to one for $\omega \approx 0.8\ \omega_0$.

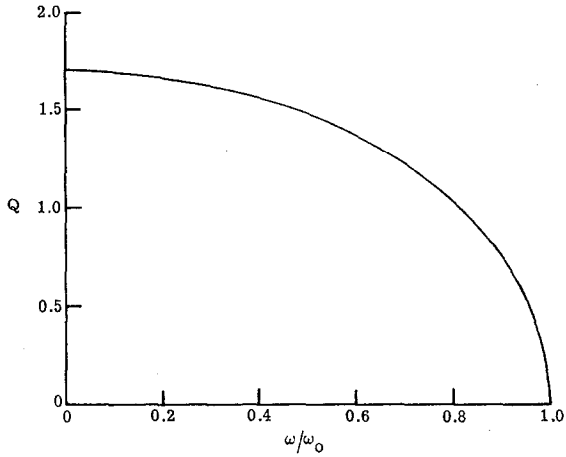

FIG. 1. Variation of $Q = \sigma_r/\sigma_{r,\min}$ with ω for the uniformly rotating disk of stars.

IV. RESULTS

The results presented in this section were obtained with an 128 × 128 active mesh for the potential calculations. The disks consisted of 100 000 stars and there

were 200 time steps per rotation. An estimate of the binary collision time for the model has been made previously [6]. The ratio of the collision time τ_c to the rotational period $\tau_r = 2\pi/\omega_0$ was estimated to be

$$\tau_c/\tau_r = 0.052N(D_{\min}/R),$$

where N is the number of stars in the system and $D_{\min}/R$ is the ratio of the grid size used in the calculations to the radius of the disk. For the present calculations we obtain

$$\tau_c/\tau_r \cong 160,$$

so that the system can be considered collisionless for about 160 rotations.

The case of a cold disk $\omega = \omega_0$ was previously investigated [2] and, as expected, the disk was found to be violently unstable. Presently we have investigated disks with $\omega = 0.8\omega_0$, $\omega = 0.6\omega_0$, $\omega = 0.4\omega_0$ and $\omega = 0$ corresponding to initial values of Q given by $Q = 1.01$, $Q = 1.35$, $Q = 1.55$, and $Q = 1.69$, respectively, where Q is given by Eq. (20). We should emphasize that the model galaxies represented by Eq. (17) do not represent a mass or velocity distribution that one would expect to find in nature. For example, for the maximum velocity at a given radius

$$V_{\max} = \sqrt{(\omega_0^2 - \omega^2)(R^2 - r^2)},$$

$f(r, v_r, v_\theta)$ as given by Eq. (17) is actually singular, and $f(r, v_r, v_\theta)$ increases with increasing v_r or v_θ. However, presently there are no really "good" stationary solutions of the collisionless Boltzmann equation available for disk galaxies. Some interesting solutions for self-gravitating disk-like stellar systems are discussed by Miyamoto [15].

The evolution of four disks of stars corresponding to Eq. (17) with (a) $\omega = 0.8\omega_0$, (b) $\omega = 0.6\omega_0$, (c) $\omega = 0.4\omega_0$, and $\omega = 0$ is presented in Fig. 2. Each of the 100 000 stars in the simulation represents 0.84×10^6 solar masses so that the total mass of the disk galaxy is $0.84 \times 10^{11} M_0$ (solar masses). The rectangular border enclosing the disks represents the active 128×128 array of cells used in the calculations. The initial radius of the disks is 16 kpc (kiloparsec). Since the disks become progressively more stable as the initial velocity dispersion is increased (or ω is decreased), the evolution of the more stable systems is investigated for longer times. The times shown in Fig. 2 and in all subsequent figures are in units of the rotational period of the cold (zero velocity dispersion) disk $\tau_r = 2\pi/\omega_0$. Figure 2(a) shows that, for $Q = 1$ (or $\omega = 0.8\omega_0$), the system is unstable and within two rotations it has formed a bar-shaped structure. After three rotations this structure remains essentially unchanged. It should be noted that all small-scale instabilities which occurred in the cold disk [2] have been stabilized. Only the large-scale

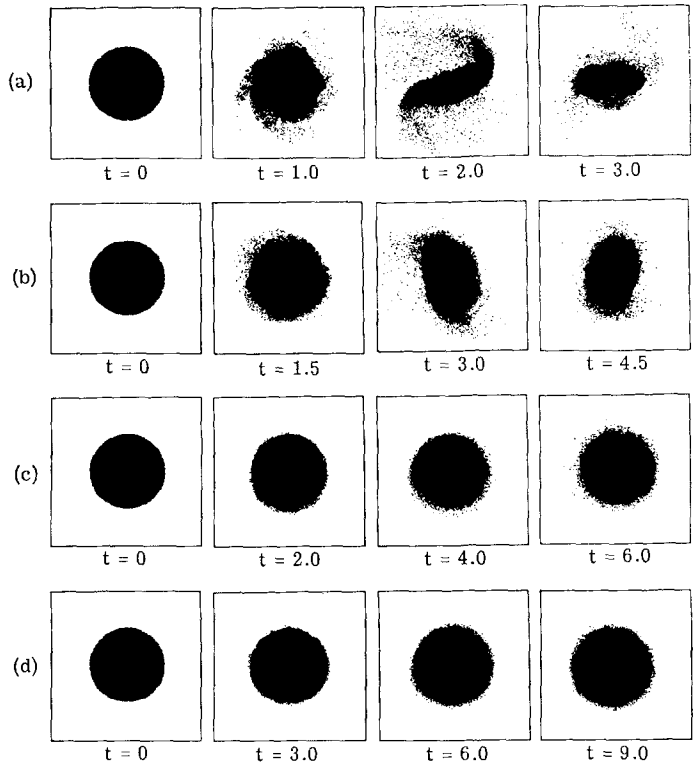

FIG. 2. Evolution of an initially uniformly rotating and stationary disk galaxy for four values of the angular velocity given by (a) $\omega = 0.8\omega_0$, (b) $\omega = 0.6\omega_0$, (c) $\omega = 0.4\omega_0$, and (d) $\omega = 0$, where ω_0 is the angular velocity of the cold (zero velocity dispersion) disk.

"bar making" instability is present. A similar result is shown in Fig. 2(b) for $Q = 1.35$. However, the bar structure is now much less pronounced. For $Q = 1.55$, the system is essentially stable. Some of the stars near the edge of the disk tend to escape to larger radii. This is to be expected since the distribution function $f(r, v_r, v_\theta)$ is singular at the edge and star orbits tend to be unstable there. Similar results are obtained for the nonrotating disk shown in Figure 2(*d*). Figure 2 indicates that the disk becomes stable for values of Q somewhere between 1.35 and 1.55 or for values of ω between $0.4\omega_0$ and $0.6\omega_0$. These results are in agreement with a normal mode analysis performed by Kalnajs (11) who finds that the simple mode corresponding to the bar disturbance becomes unstable for $\omega \gtrsim 0.508$.

Four individual star orbits for each of the four disks of stars are given in Fig. 3. Figures 3(a) and 3(b) indicate that the orbits are quite perturbed because of the changing structure of the disk. The orbits in Figs. 2(c) and 2(d) are nearer to

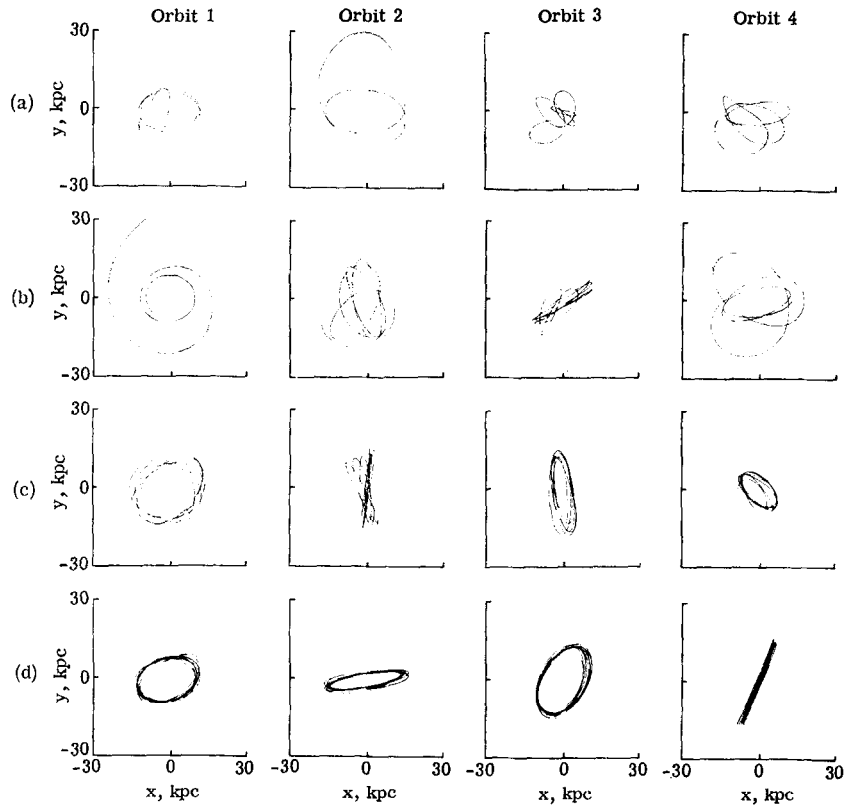

FIG. 3. Orbits of four individual and randomly chosen stars corresponding to the four initial conditions shown in Fig. 2. The time during which the orbits are plotted corresponds to the times shown in Fig. 2.

unperturbed orbits and indicate that only small fluctuations occur as the disks evolve.

The evolution of the distribution of the radial velocities of the stars as a function of star radius is shown in Fig. 4. As can be seen from Fig. 4(a) and (b), the radial velocities of the stars increase rapidly as the system evolves. Also, a large number of stars greatly increase their radii. For $\omega = 0.4\omega_0$ and $\omega = 0$, the results in Fig. 4(c) and (d) show that there is little increase in the radial velocities, which, of course, were already large at $t = 0$. Only a few stars increase their radii beyond the initial disk radius, especially for the disk in Fig. 4(d). Nevertheless the distribution of radial velocities at $t = 3$ in Fig. 4(d) shows that quite subtle changes take place in the velocity distribution near the edge of the disk. However, these changes do not appear to affect the structure of the disk appreciably. Similar results are shown

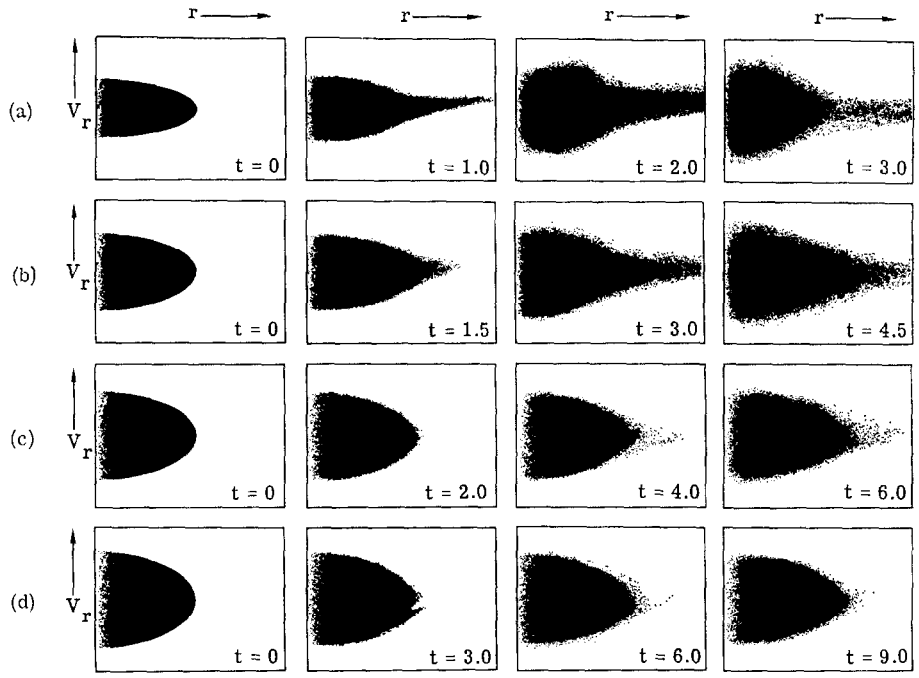

FIG. 4. Evolution of the radial velocity components of the stars plotted as a function of radius for the four disks shown in Fig. 2.

in Fig. 5 for the azimuthal velocity components of the stars. The rectangular borders enclosing the velocity distributions in Figs. 4 and 5 extend from −350 km/sec to 350 km/sec and from 0 to 30 kpc.

In order to obtain more quantitative information than can be obtained from Figs. 2 to 5, the disk is divided into a number of concentric rings, each of 1/2 kpc width. The radial dependence of various parameters averaged azimuthally over each ring is then obtained. Figure 6 shows the evolution of the rms radial velocity dispersion obtained in the above manner for the four disks under investigation. Figure 6(a) shows rather large changes in the rms radial velocities of the disk, with a pronounced increase in the velocity dispersion as the disk evolves. Similar but less pronounced changes occur for the disk in Fig. 6(b) and (c). The central rms radial velocities of the stars actually decrease slightly for the nonrotating disk shown in Fig. 6(d). A better indication of how hot a disk of stars becomes can be obtained from the evolution of $Q = \sigma_r/\sigma_{r,\min}$. Figure 7 shows the evolution of the azimuthally averaged Q for the four disks. The results in Fig. 7(a) indicate that the disk becomes rather hot, with values of Q in the outer parts of the disk near six. For the disk with an initial angular velocity of $\omega = 0.6\omega_0$, the value of Q

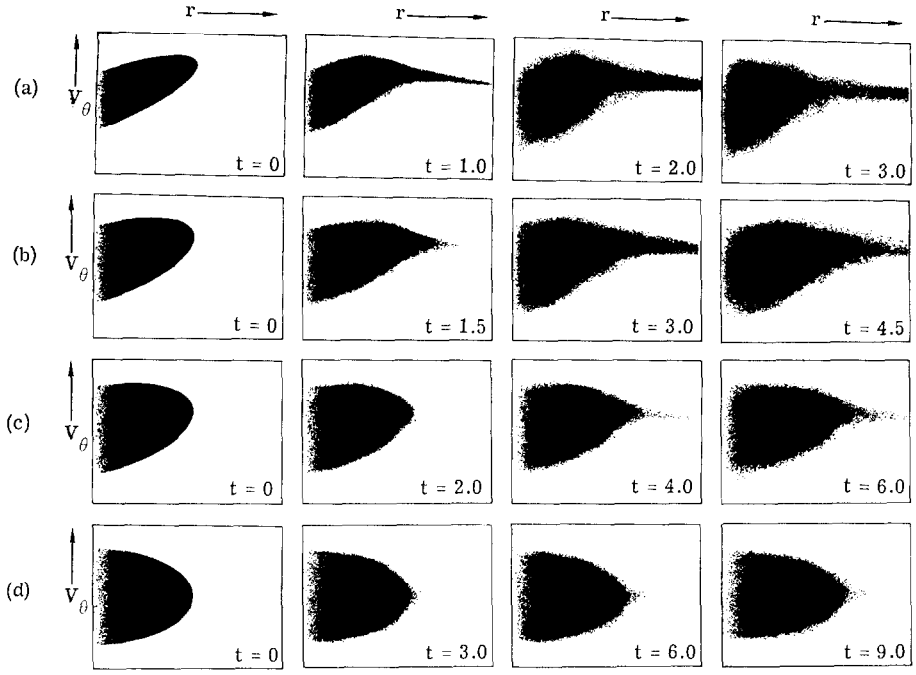

FIG. 5. Evolution of the azimuthal velocity components of the stars plotted as a function of radius for the four disks shown in Fig. 2.

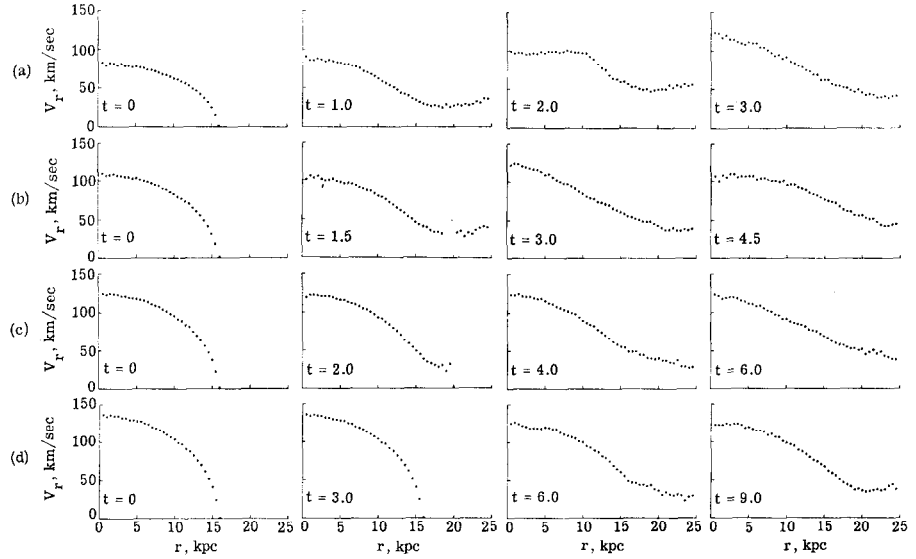

FIG. 6. Evolution of the rms radial velocities of the stars as a function of radius for the four disks shown in Fig. 2.

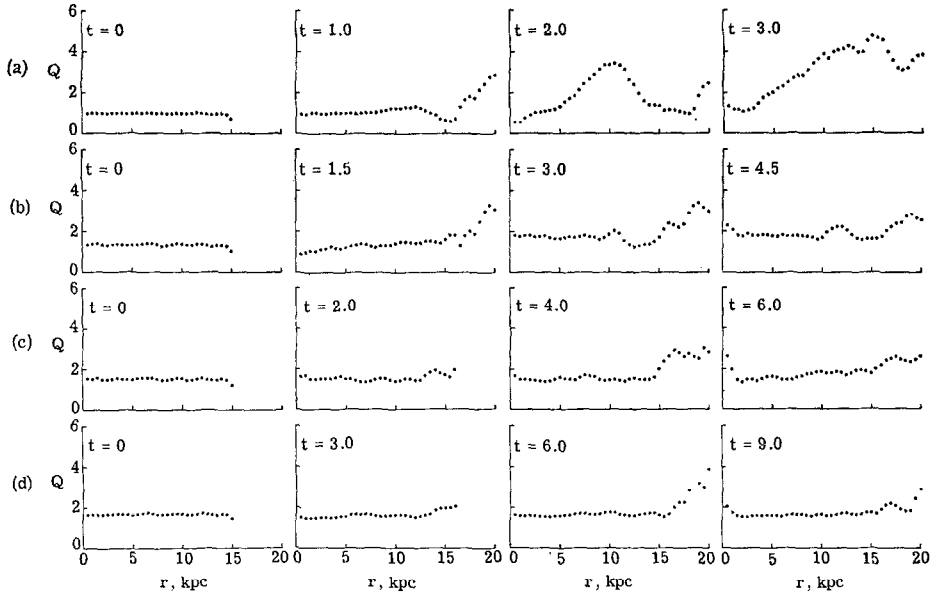

FIG. 7. Evolution of $Q = \sigma_r/\sigma_{r,\min}$ for the four disks shown in Fig. 2.

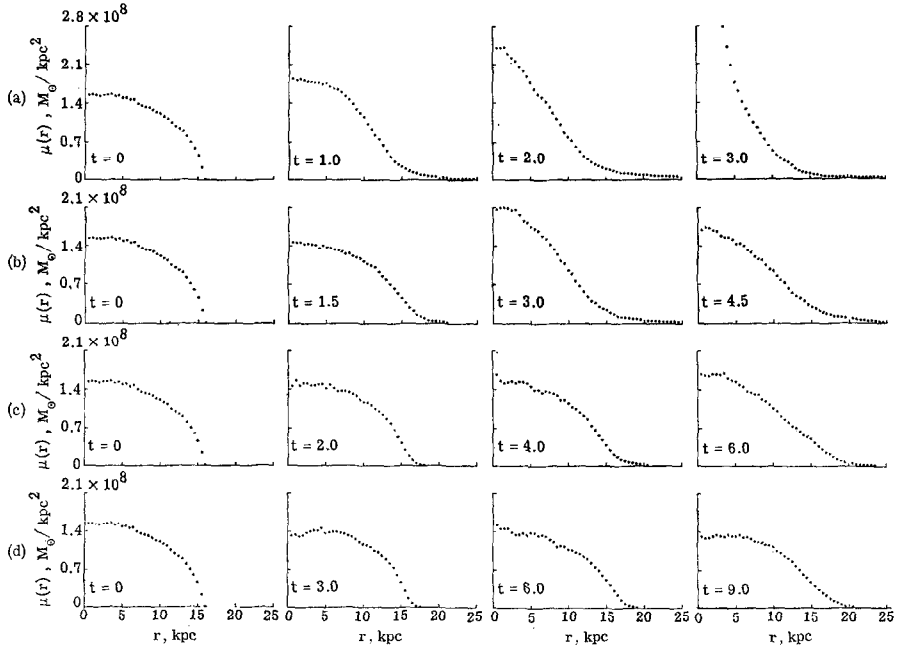

FIG. 8. Evolution of the azimuthally average density for the four disks shown in Fig. 2.

increases from 1.35 to about 2. Smaller increases occur for the disk in Fig. 7(c). Finally, the value of Q in Fig. 7(d) for the nonrotating disk remains nearly constant at $Q = 1.69$.

The evolution of the azimuthally averaged density for the four disks is presented in Fig. 8. For the most unstable disk shown in Fig. 8(a), the final central density increases to a high value given by an approximately exponential density variation. Similar results were previously obtained for other violently unstable disk galaxies [6]. In Fig. 8(b) the central density oscillates between 1.4×10^8 and $2.1 \times 10^8 M_\odot/\text{kpc}^2$, reaching a final value of about $1.7 \times 10^8 M_\odot/\text{kpc}^2$ after 4.5 rotations. The changes in the density for the disk shown in Fig. 8(c) were the least pronounced of the four disks. For the nonrotating disk in Fig. 8(d) the central density appears to be oscillating near the value of 1.4×10^9 $M_\odot/\text{kpc}^2$. When the kinetic energy of the disks is plotted as a function of time, it is found that the kinetic energy initially oscillates nearly sinusoidally about the equilibrium value. The initial amplitude of the oscillations is about 5% of the equilibrium value and the period of the oscillations in all four cases is near the rotational period of the cold balanced disk. For disks (a) and (b), the oscillations are strongly damped after the first two oscillations. For disk (c), the oscillations are more slowly damped whereas for disk (d) the oscillations in the kinetic energy show no damping during the nine rotations investigated

SUMMARY

The evolution of a disk galaxy which is a stationary solution of the collisionless Boltzmann equation is investigated for four values of the initial rms velocity dispersion or initial rotational velocity of the disk. For rotational velocities of $\omega = 0.8\omega_0$ and $\omega = 0.6\omega_0$ (ω_0 is the rotational velocity of the cold, zero velocity dispersion disk) corresponding to $Q = 1$ and 1.35, respectively, the disk formed a bar-like structure. For $\omega = 0.4\omega_0$ and $\omega = 0$ (or $Q = 1.55$ and $Q = 1.69$), the disk was essentially stable; however, for these two cases the disks sustained what appear to be natural oscillations or pulsations with a period near the rotational period of the cold balanced disk. The pulsations were especially pronounced for the nonrotating disk where they did not show a decrease in amplitude for the nine rotations investigated,

ACKNOWLEDGMENTS

The author would like to thank Dr. G. Rybicki for suggesting the improvement of the potential solver and Prof. A. Toomre and Dr. A. Kalnajs for numerous suggestions.

REFERENCES

1. R. H. MILLER AND K. H. PRENDERGAST, *Ap. J.* **151** (1968), 699.
2. F. HOHL AND R. W. HOCKNEY, *J. Computational Phys.* **4** (1969), 306.
3. J. W. COOLEY AND J. W. TUKEY, *Math. Comp.* **19** (1965), 297.
4. R. H. MILLER, K. H. PRENDERGAST, AND W. J. QUIRK, *Ap. J.* **161** (1970), 903.
5. R. W. HOCKNEY AND F. HOHL, *Astronom. J.* **74** (1969), 1102.
6. F. HOHL, "Dynamics of Disk Galaxies," NASA TR R-343, 1970.
7. R. W. HOCKNEY, "Methods of Computational Physics," **9** (1970), 135, Academic Press, New York.
8. S. CHANDRASEKHAR, "Principles of Stellar Dynamics," Dover, 1960.
9. J. H. JEANS, *Mon. Not. R. Astro. Soc.* **76** (1915), 70.
10. K. C. FREEMAN, *Mon. Not. R. Astro. Soc.* **134** (1966), 15.
11. A. J. KALNAJS, private communication, 1970.
12. A. TOOMRE, *Ap. J.* **139** (1964), 1217.
13. W. H. JULIAN, *Ap. J.* **155** (1969), 117.
14. A. J. KALNAJS, *Ap. J.* **166** (1971), 275.
15. M. MIYAMOTO, *Pulb. Astr. Soc. Jap.* **23** (1971), 21.